Astron. Astrophys. 324, 1115–1122 (1997)

ASTRONOMY
AND
ASTROPHYSICS

Polarization models of filamentary molecular clouds

Per Carlqvist[1] **and Helmuth Kristen**[2]

[1] Alfvén Laboratory, Royal Institute of Technology, S-100 44 Stockholm, Sweden
[2] Stockholm Observatory, S-133 36 Saltsjöbaden, Sweden

Received 8 March 1996 / Accepted 19 November 1996

Abstract. We study numerically the linear polarization and extinction of light from background stars in three types of models of elongated molecular clouds by following the development of the Stokes parameters. The clouds are assumed to be of cylindrical shape and penetrated by a helical magnetic field $\boldsymbol{B}$. In the first two models we study only the relative magnitude of the polarization assuming that the polarization is proportional to B^{μ}, where primarily $\mu = 2$. Provided there is no background/foreground polarization present we find from the cylindrically symmetric Model I that the angle of polarization has a bimodal character with the polarization being either parallel with or perpendicular to the axis of the filament. For some magnetic-field geometries both angles may exist in one and the same filament. It is concluded that it is not a straightforward task to find the magnetic-field-line pattern from the polarization pattern. If a background/foreground polarization exists or, as in Model II, the filament is not cylindrically symmetric, the bimodal character of the angle of polarization is lost. By means of Model III we have, using semi-empirical methods based on the Davis–Greenstein mechanism, estimated the absolute degree of polarization in the filamentary molecular cloud L204. It is found that the polarization produced by the model is much less than the polarization observed. We therefore conclude that most of the polarization measured in the L204 cloud is not produced in the cloud itself but is constituted by a large-scale background/foreground polarization.

Key words: ISM: clouds – ISM: general – ISM: individual objects: L204 – ISM: magnetic fields – physical data and processes: polarization

1. Introduction

Dark molecular clouds often form elongated structures containing many intricate details. Polarimetric measurements of the light from stars behind such clouds have revealed that the polarization vectors mostly show a regular and systematic pattern although more irregular patterns also exist (Myers & Goodman 1991). The angle between the mean direction of the polarization vectors and the long axis of the dark clouds varies from one cloud to another and may adopt any value from being parallel with the projected cloud elongation (e.g. L1755 (Goodman et al. 1990); the eastern part of the R CrA cloud (Vrba et al. 1981); L1641 (Vrba et al. 1988)) to being perpendicular to it (e.g. B216–217 (Heyer et al. 1987; Goodman et al. 1992); L204 (McCutcheon et al. 1986); the Cha I dark cloud (McGregor et al. 1994)). Generally, the magnetic field in the clouds has been considered to be aligned with the polarization vectors.

One has attempted to interpret the elongated molecular clouds as highly flattened slabs, seen edge on, which have collapsed in one dimension along magnetic field lines (Langer 1978; Moneti et al. 1984; Tamura et al. 1987; McGregor et al. 1994). Especially in the case where the polarization vectors are fairly perpendicular to the long axis of the cloud this model may seem very simple and attractive. For clouds with polarization vectors being more parallel with the long axis the interpretation is perhaps less obvious. Moreover, the probability of finding so many molecular clouds turning edgewise may also offer a problem.

Another model suggested for the elongated molecular clouds presumes that these clouds are truly filamentary, i.e. approximately of cylindrical shape, with a helical magnetic field directed along the clouds (Alfvén & Carlqvist 1978; Carlqvist 1988). The structures of the plasma and magnetic field in this model bear some resemblance with corresponding structures in eruptive solar prominences. Evidence for helical structures has to date been found in a few molecular clouds (Carlqvist & Gahm 1992). Many experiments in laboratory plasmas also show that plasmas have a strong tendency to line up along magnetic fields and electric currents. One apparent problem with the model is that the polarization pattern observed in many of the elongated molecular clouds does not very much resemble the magnetic field geometry suggested.

The aim of the present paper is to consider this problem. Using numerical methods we shall calculate the polarization pattern of light from stars behind a filamentary molecular cloud model penetrated by a helical magnetic field. In particular we

Send offprint requests to: Per Carlqvist

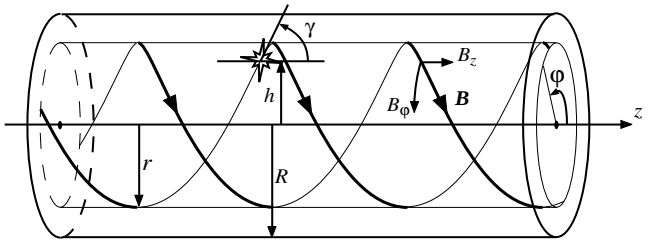

Fig. 1. Cylindrical filament of radius R penetrated by a helical magnetic field $\boldsymbol{B} = (0, B_\varphi, B_z)$. Starlight passes the filament at the distance h from the axis of the filament.

shall study the polarization pattern in a model of the elongated molecular cloud complex L204. The polarization calculated is compared with the observed polarization pattern.

2. Geometry and methods of calculation

2.1. Filamentary geometry

We consider a model of a cylindrical filament of radius R which is permeated by a helical magnetic field $\boldsymbol{B}$ (Fig. 1). With cylindrical coordinates (r, φ, z) the field may be divided into a toroidal component B_φ and an axial component B_z. The offset of the line of sight (l.o.s.) to a background star relative to the filamentary axis (z-axis) is denoted $h = r \sin\varphi$.

In general the filament is not perpendicular to the l.o.s., but is tilted by the angle α from the perpendicular direction. α is defined to be positive when the z-axis tends to point away from the observer. The apparent angle between a line parallel with the z-axis and the magnetic field is γ. Geometric considerations yield

$$\gamma = \arctan \frac{B_\varphi [1 - (h/r)^2]^{1/2}}{B_z \cos\alpha - B_\varphi (h/r) \sin\alpha} \quad . \tag{1}$$

2.2. General approach

We divide the part of the l.o.s. passing through the filament into a large number of finite elements. Each element contributes to the polarization and extinction of passing light. The magnitude of the influence depends on the density of the neutral gas and the strength and orientation of the magnetic field. The combined effect of many elements is treated by matrix calculus permitting us to numerically trace the evolution of the Stokes parameters throughout the filament.

In the interstellar medium (ISM), birefringence and circular polarization are known to be negligible compared to linear polarization (Serkowski et al. 1967). Hence, we shall consider only linearly polarized light. Furthermore, the linear polarization is small in the ISM so that $P = P(\%)/100 \ll 1$.

2.3. Properties of the elements

We study a polarizing element of thickness ds and with linear extinction coefficients $2\sigma_1$ and $2\sigma_2$, the indices referring to the principal axes of maximum and minimum opacity, respectively. With $\delta = \sigma_1 + \sigma_2$ and $\Delta\sigma = \sigma_1 - \sigma_2$, the effect of the element on the Stokes parameters I, Q, U, V (vector $\boldsymbol{C}_{sky}$), referring to infalling light, is described by

$$\frac{\mathrm{d}\boldsymbol{C}_{sky}}{\mathrm{d}s} = \mathsf{H}_{sky} \cdot \boldsymbol{C}_{sky} \tag{2}$$

$$\mathsf{H}_{sky} = \begin{bmatrix} -\delta & \Delta\sigma\cos 2\zeta & \Delta\sigma\sin 2\zeta & 0 \\ \Delta\sigma\cos 2\zeta & -\delta & 0 & 0 \\ \Delta\sigma\sin 2\zeta & 0 & -\delta & 0 \\ 0 & 0 & 0 & -\delta \end{bmatrix} \tag{3}$$

neglecting birefringence (cf. Martin 1974). Here ζ is the orientation of the principal axis of maximum transmissivity of the element with respect to the z-axis. Throughout this paper the contribution to polarization is assumed to be parallel with the direction of the ambient magnetic field. Hence, we can identify ζ with γ in Eq. (1).

For a given magnetic field strength, the contribution to polarization is maximized if the magnetic field is oriented perpendicular to the l.o.s. Should the magnetic field have a component aligned with the l.o.s., the maximum contribution to polarization is reduced by a factor corresponding to the square of the relative projection of the magnetic field vector η (cf. Martin 1975),

$$\eta^2 = \left[\cos\psi\cos\alpha - \frac{h}{r}\sin\psi\sin\alpha\right]^2 + \left[1 - \left(\frac{h}{r}\right)^2\right]\sin^2\psi \tag{4}$$

where ψ is the angle between the B_z component and $\boldsymbol{B}$.

From the Stokes parameters we may derive the degree of polarization P and the angle of polarization θ, defined as the angle between the projection of the z-axis and the polarization vector. Since $\theta = 1/2 \arctan(|U|/Q) \pm n \cdot 90°$, where n is an optional integer, one must keep in mind that this expression considers both the direction of minimum and maximum intensity.

3. Model I

3.1. Properties of the model

We shall first study the polarization of light in a simple and cylindrically symmetric model of a filamentary molecular cloud penetrated by a helical magnetic field $\boldsymbol{B}$. The model consists of a cylindrical cloud of radius R with the constant gas density n_g. Here we are only interested in a model comprising a general helical magnetic field. Hence, we consider a very simple helical field having the components

$$B_\varphi = B_{\varphi 0} \frac{r}{R} \tag{5}$$

$$B_z = B_{z0} \tag{6}$$

where B_{z0} and $B_{\varphi 0}$ are constants. By choosing the parameter

$$\kappa = B_{z0}/B_{\varphi 0} \tag{7}$$

properly the field can be varied from a pure toroidal field, over a helical field, to a homogeneous field aligned with the z-axis.

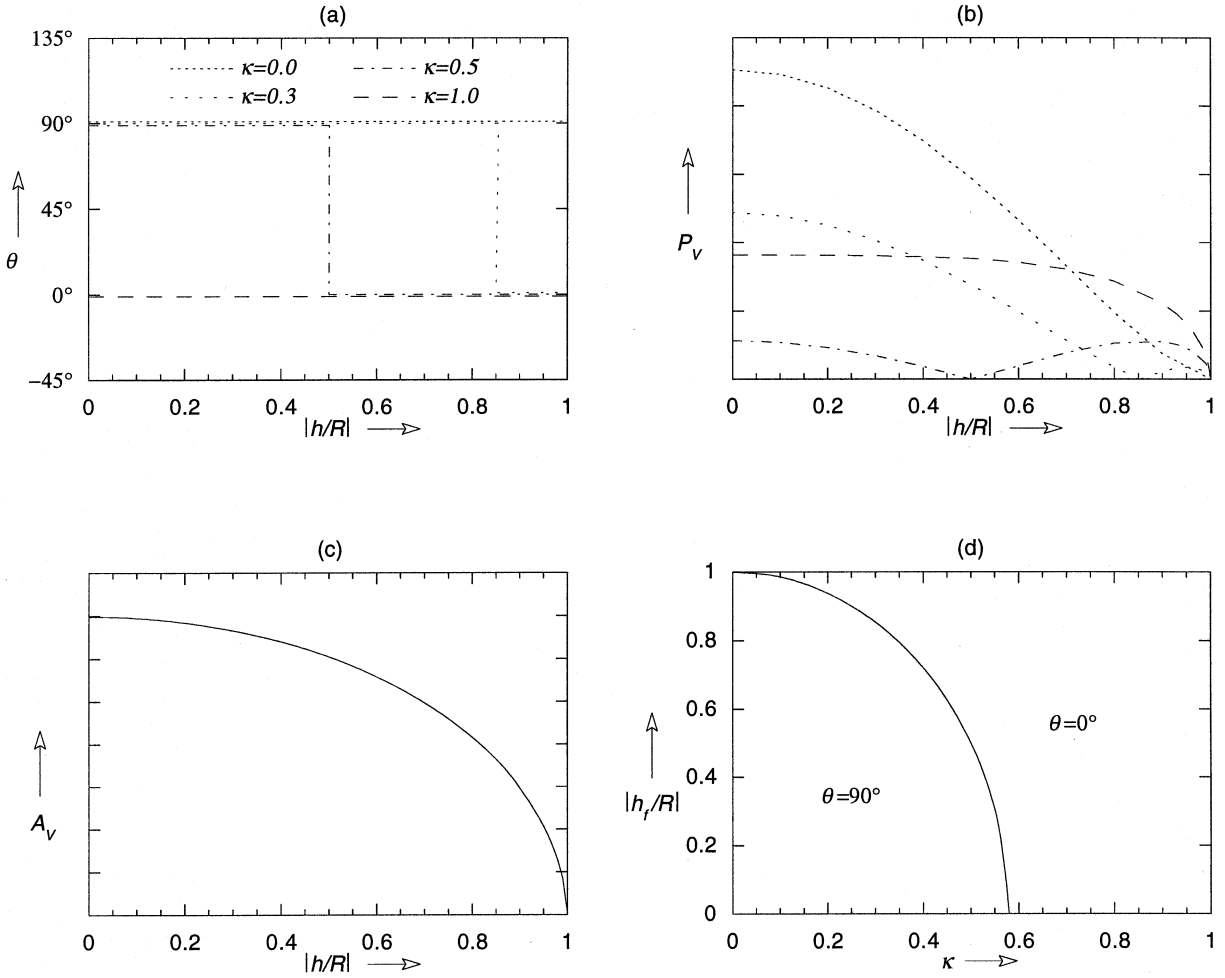

Fig. 2a–d. Angle of polarization θ, polarization P_V, and extinction A_V (mag) in a Model I filament shown as functions of $|h/R|$ in **a**, **b**, and **c**, respectively. In **d** the position of the flip $|h_f/R|$ is illustrated as a function of κ. The scales of the polarization and extinction are arbitrary. It is assumed that $\alpha = 0^\circ$ and that there is no background/foreground polarization.

In the present model we shall not adopt any special polarization mechanism but only assume that $\Delta\sigma$ is proportional to B^2 (cf. Sect. 5.3). Further, we shall not be concerned with the absolute magnitudes of the polarization and extinction. We let the average opacity of the element be $\delta \mathrm{d}s = bn_g \mathrm{d}s$ where b is a proportional constant. The quantity $\Delta\sigma$ is directly related to the polarization efficiency of the element through $\Delta\sigma = pB^2\eta^2 n_g$ where p is a proportional constant. In order to facilitate a comparison of filaments with different κ-values we let the magnitude of the magnetic field be constant at $r/R = 0.5$ for all κ.

3.2. Filament perpendicular to the line of sight, $\alpha = 0^\circ$

Considering first a filament that is perpendicular to the l.o.s. ($\alpha = 0^\circ$) we have numerically calculated the degree of polarization P_V, the angle of polarization θ, and the extinction of light A_V in the filament. These parameters are shown in Fig. 2 a,b,c as functions of $|h/R|$ for a few different κ-values. It is assumed that there is no external polarization. Since the projection of the magnetic field on the celestial sphere is here symmetric with respect to $h = 0$ the quantities θ, P_V, and A_V are also symmetric with respect to $h = 0$.

A striking feature of the polarization pattern in the filament is that the angle of polarization θ is either 0° or 90°. It is of particular interest to note that for $\kappa = 0.3$ and 0.5 the polarization angle changes abruptly from 90° to 0° as $|h/R|$ is increased. For $\kappa = 0$ and 1 there is no flip and $\theta = 90^\circ$ and 0°, respectively, everywhere in the filament. The normalized position of the flip, $|h_f/R|$, is given as a function of κ in Fig. 2d. It is found that the flip occurs only in the interval $0 < \kappa < 0.58$.

Figs. 2 a,b show that the polarization tends to zero at those very positions $|h| = h_f$ where there is a flip in θ. This means that elements situated along the l.o.s. passing through $|h| = h_f$ contribute as much to the polarization parallel to the filament as to the polarization perpendicular to it.

It should be noted that for $\kappa = 0.5$ the polarization in most of the filament is considerably reduced compared with the polarization typically obtained for the other values of κ shown in Fig. 2. The contributions to the polarization from the elements

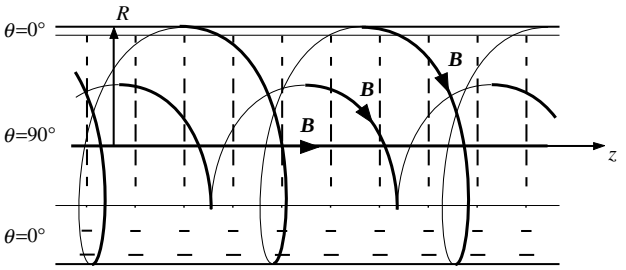

Fig. 3. Polarization map of a Model I filament with no background/foreground polarization and $\kappa = 0.3$, $\alpha = 30°$. It is to be noted that the borderlines separating the two polarization angles are non-symmetric with respect to the axis of the filament. The scale of the polarization is arbitrary.

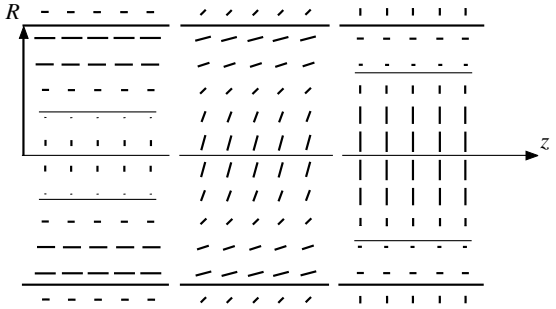

Fig. 4. Polarization map of a Model I filament with a finite background/foreground polarization and $\kappa = 0.5$, $\alpha = 0°$. The angles of the background/foreground polarization are $\theta_b = 0°$, 45°, and 90°. The scale of the polarization is arbitrary.

along the l.o.s. then have a particularly strong tendency to cancel one another. One important reason for this is that the flip occurs about half-way between the axis and the edge of the filament.

3.3. Oblique filament, $\alpha \neq 0°$

If the filament is not perpendicular to the l.o.s. ($\alpha \neq 0°$) the projection of the magnetic field on the celestial sphere is not any more symmetric with respect to the axis of the filament. In this case we may expect that neither the polarization P_V nor the angle of polarization θ, as functions of h/R, are symmetric with respect to $h = 0$. This is confirmed by Fig. 3 showing the polarization pattern for a filament where $\alpha = 30°$ and $\kappa = 0.3$. It is clear that also here θ adopts only one of the two angles 0° and 90°. Again θ may flip between these two values but the positions of the flips are not the same as for $\alpha = 0°$ and they are not symmetric with respect to $h = 0$.

Included in Fig. 3 are also the projections of a few magnetic field lines. As can be seen from the figure, the polarization pattern differs drastically from the magnetic field line pattern. We may therefore conclude that, given the polarization pattern, it is not an easy task to figure out the structure of the magnetic field.

The bimodal character of the polarization pattern discussed above is an important property of the model studied. It depends on the cylindrical symmetry of the filament and may be explained as follows. When we are dealing with polarizing elements in the filament, which both separately and taken together represent polarizations that are small compared with unity, the resulting polarization does not depend on the order in which we put the elements. Hence, we may pair elements that are situated symmetrically with respect to the centre of the path of light through the filament. Each of these pairs would transform unpolarized infalling light into polarized light with the angle of polarization equal to either 0° or 90°. A summation of the contributions from all the pairs in the filament can only result in a final angle of polarization of either 0° or 90° in case of unpolarized infalling light.

Bimodal polarization patterns similar to those obtained in the present model have also been observed in a few molecular clouds (see Sect. 6).

3.4. Background and foreground polarization

We now consider a situation where the light penetrating the filament is also partly polarized by the ISM outside the filament. It is irrelevant to the result whether the external polarization takes place in front of or behind the filament. Fig. 4 shows the polarization pattern in a filament where $\kappa = 0.5$ and $\alpha = 0°$ and where the background/foreground polarization forms the angles $\theta_b = 0°$, 45°, and 90° with the axis of the filament.

When $\theta_b = 90°$ it is seen that, just as in the case of no background/foreground polarization, the pattern of polarization is symmetric with respect to $h = 0$ and that the angle of polarization adopts only the values 0° and 90°. Flips now occur further away from the axis of the filament at $h_f/R = \pm 0.65$. If the background/foreground polarization is sufficiently large no flips at all are present and $\theta = 90°$ everywhere in the filament.

When $\theta_b = 0°$ the polarization pattern is similar to that when $\theta_b = 90°$ but the flips are now closer to $h = 0$ at $h_f/R = \pm 0.33$. For a large enough background/foreground polarization the flips again disappear.

When $\theta_b = 45°$ there are no flips in θ. Instead, the angle of polarization changes smoothly with h/R. Studies including other values of θ_b show that flips may occur only if θ_b is 0° or 90°. However, rapid transitions of θ between 0° and 90° may take place if either θ_b is close to 0° or 90° or the background/foreground polarization P_{Vb} is small compared with the polarization caused by the filament.

We have also studied the polarization in the filament for various combinations of α, κ, and external polarization on the assumption that $\Delta\sigma$ is proportional to B^μ where $\mu = 0$, 1, 3. Also in these cases the angle of polarization is either 0° or 90° provided there is no background/foreground polarization.

4. Model II

Above we have considered filaments which are cylindrically symmetric. It may also be of some interest to study the polarization in filaments where such a symmetry does not prevail. Here we adopt a model comprising a magnetic field that is not

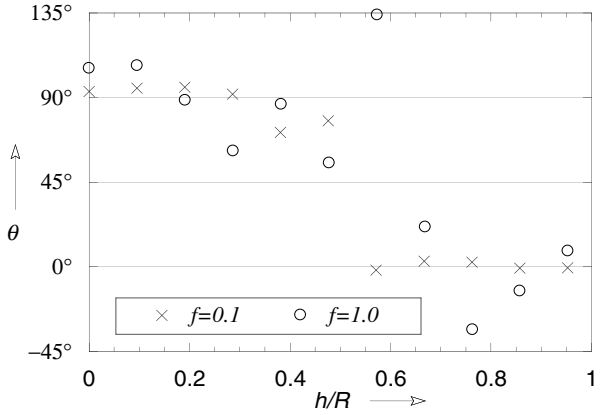

Fig. 5. Angle of polarization θ as a function of h/R in a Model II filament where the strength of the helical magnetic field varies partly at random from one flux element to another. It is assumed that $\kappa = 0.5$, $\alpha = 0°$, and that there is no background/foreground polarization. The crosses refer to a relatively small degree of randomness while the circles refer to a larger degree of randomness.

cylindrically symmetric. A certain degree of randomness and discreteness is also introduced into the field.

We consider a filament that consists of many helical subfilaments of different magnetic field strengths. We let the part of the l.o.s. passing through the filament be divided into a number of equally wide elements (corresponding to the subfilaments) where the magnetic field adopts a discrete value in each of the elements. The magnetic field has the components

$$B_\varphi = B_{\varphi 0}(1 + f\nu)\frac{r}{R} \tag{8}$$

$$B_z = B_{z0}(1 + f\nu) \tag{9}$$

where r is the radius of the central position of the element, ν is a random number in the interval -1 to 1, specific for the element, and f is a factor determining the degree of randomness. The magnetic field, which has the same helical shape as that in Model I, is thus composed of one part that behaves regularly and another part which is random and hence non-symmetric. As before it is supposed that the density of the gas in the filament is constant and that $\Delta\sigma$ is proportional to B^2.

Fig. 5 shows two examples of the variation of θ in a filament with no background/foreground polarization and where $\kappa = 0.5$, $\alpha = 0°$, and $f = 0.1$ and 1.0. The number of elements that goes into the diameter of the filament is chosen to be 21 so that the width of each element is approximately 0.095 R. It is clear from the figure that, when symmetry is broken, the angle of polarization is not any more limited to 0° or 90° but is instead scattered around these values. For $f = 0.1$ the scatter is relatively small, about 9° in the interval $0 \leq h/R \leq 0.4$ and about 1.6° in the interval $0.6 \leq h/R \leq 1$. Between these intervals there is a transition region that corresponds to the flip. Hence, there is an obvious similarity to Fig. 2a in this case. For $f = 1.0$ the scatter is larger but still there is a clear tendency of concentration of the θ-values to 90° for $0 \leq h/R \leq 0.4$ and to 0° for $0.6 \leq h/R \leq 1$. Also the polarization is subject to scatter when f departs from zero.

5. Model III

5.1. The polarization mechanism

In the models treated above only the relative degrees of polarization and extinction have been considered. Now we shall turn to a more quantitative description of the polarization and extinction using the classic Davis–Greenstein mechanism based on spinning and magnetically aligned grains (Davis & Greenstein 1951) with further refinements by Jones & Spitzer (1967) and by Greenberg (1978). The ratio of the time scales for collisional relaxation and paramagnetic relaxation of the spin axes of the grains can here be expressed as

$$\delta = \frac{\tau_c}{\tau_m} = \frac{\chi''}{\omega}\frac{B^2}{2an_g}\left(\frac{2\pi}{m_g k T_g}\right)^{1/2} \tag{10}$$

where χ'', ω, and a are the imaginary part of the magnetic susceptibility, the angular spin velocity, and the radius of the grains, and m_g and T_g are the mass and temperature of the ambient gas particles, respectively.

Furthermore, the parameter of orientation of the grains is given by

$$\xi = \left[\frac{1 + \delta(T_i/T_g)}{1 + \delta}\right]^{1/2} \tag{11}$$

where T_i is the grain temperature. We are here mainly interested in situations where $T_g/T_i > 1$ and thereby $\xi < 1$. Using the reduction factor $R(\xi) = P_V(\xi)/P_V(0)$ given by Greenberg (1969) and the usual relations between the extinction A_V, colour excess $E(B-V)$, and total column density of neutral hydrogen $N(H_{tot})$ (Bohlin et al. 1978) we obtain

$$P_V(\xi) = 5.3 \times 10^{-22} R(\xi) N(H_{tot}) \frac{P_V(0)}{A_V} \tag{12}$$

where the value of the ratio $P_V(0)/A_V$ depends on the model of the grains adopted. For a core-mantle model Greenberg (1978) found a value of 0.16 for $P_V(0)/A_V$ while for bare silicate spheroids of a few different shapes Kim & Martin (1995) considered values in the range 0.03 – 0.18. Eq. (12) gives the polarization in a column of homogeneous magnetic field and constant gas density.

Since long it has been recognized that the Davis–Greenstein mechanism, with $\chi'' = 2.5 \times 10^{-12}\omega/T_i$ (e.g. Spitzer 1978; Greenberg 1978) and ω of the order of 10^5 rad s^{-1}, is not efficient enough to account for the polarization observed in the ISM. As a result of the search for a more efficient polarization mechanism it has been suggested that the grains may be subject to suprathermal rotation (Purcell 1979) and/or superparamagnetic damping (Spitzer & Tukey 1951; Jones & Spitzer 1967; Mathis 1986). For the latter mechanism to occur the grains must contain small clumps of some material which substantially enhances the value of χ''. Some evidence for such clumps has

recently been given by Goodman & Whittet (1995) and Martin (1995).

Here we shall not further discuss the possible physical reasons for the comparatively high polarization efficiency of the ISM. Instead we shall assume that the basic Davis–Greenstein mechanism is on the whole valid and put

$$\chi'' = 2.5 \times 10^{-12} C_1 \frac{\omega}{T_i} \tag{13}$$

where C_1 is a correction factor which is to be empirically estimated.

5.2. The correction factor C_1

We shall estimate the value of C_1 using the upper limit of the polarization efficiency, $P_{max}/\tau_V = 0.028$, found by Serkowski et al. (1975) in their study of the polarization of a large number of stars. Main contributors to the polarization and extinction in the ISM are those media which contain dust and gas, i.e. the warm neutral medium (WNM), the cold neutral medium (CNM), and molecular clouds. From Eqs. (10) – (12) it is seen that the polarization is preferentially favoured by a small gas-grain collision frequency, and hence a low gas density. The WNM is therefore the most efficient polarizer out of the three media while the molecular cloud is the least efficient.

For the maximum polarization efficiency to be reached it is required that the polarization and extinction conditions in the ISM are extremely favourable. This means that there should be a relatively large proportion of WNM and probably no molecular clouds along the l.o.s. representing the maximum polarization efficiency. The ratio of the masses of the WNM and the CNM in the local ISM is found to be in the range $(n_g f_\nu)_{WNM}/(n_g f_\nu)_{CNM} \approx 0.15 - 0.35$ (e.g. Spitzer 1985; Kalberla et al. 1985; Kulkarni & Heiles 1987; Brinks 1990; Knapp 1990; and references therein). For our calculation of C_1 we adopt $(n_g f_\nu)_{WNM}/(n_g f_\nu)_{CNM} = 0.3$, in the upper part of this range. Furthermore, we put $n_g = 0.3\,\mathrm{cm}^{-3}$ and $T_g = 8000\,\mathrm{K}$ for the WNM, $n_g = 20\,\mathrm{cm}^{-3}$ and $T_g = 100\,\mathrm{K}$ for the CNM, $T_i = 10\,\mathrm{K}$, and $a = 0.12\,\mu\mathrm{m}$. Using Greenberg's value of $P_V(0)/A_V = 0.16$ we find that the polarization efficiency attains the observed maximum value for $C_1 \approx 10$ if the magnetic field is $B = 3\,\mu\mathrm{G}$ or for $C_1 \approx 4$ if $B = 5\,\mu\mathrm{G}$. It is assumed that the magnetic field is homogeneous and perpendicular to the l.o.s. Choosing a value approximately in the middle of the interval given by Kim & Martin (1995), $P_V(0)/A_V = 0.08$, we obtain $C_1 \approx 18 - 48$ for the same magnetic fields. For values of $P_V(0)/A_V$ in the lower part of the interval ($\lesssim 0.05$) the observed maximum polarization efficiency cannot at all be attained. Since, in the following, we do not want to underestimate the polarization we shall be conservative and use the C_1-values connected with the lower value of the interstellar magnetic field.

5.3. Polarization in a model of the L204 molecular cloud complex

Using Eq. (12) we shall quantitatively study the polarization in a model of the filamentary molecular cloud complex L204. The L204 complex constitutes an elongated ($\sim 4^\circ$) molecular cloud with a mass of $\sim 400\,\mathrm{M}_\odot$ at a distance of $\sim 170\,\mathrm{pc}$ (McCutcheon et al. 1986; hereafter MVDC). From velocity data MVDC argue that the geometry of the cloud is not sheetlike but instead must be filamentary. In the more dense parts of the filament around $\delta(1950) \approx -12^\circ\,00'$ the linear mass density is $24 - 28\,\mathrm{M}_\odot$ per $10'$ along the filament (MVDC) while the extinction is at least 6 mag (Lynds 1962). MVDC have measured the polarization of light of background stars in the outer parts of the filament ($A_V \lesssim 2.5\,\mathrm{mag}$). These measurements show that the polarization vectors are predominantly perpendicular to the filament with a mean polarization of about $P(\%) = 2.3\%$. This is very similar to the conditions in the neighbourhood of the filament where the position angle of the polarization is approximately the same and the mean polarization is about two percent (see Fig. 3 in MVDC and references therein).

For our study we consider a very simple model of the L204 cloud in the form of a cylindrically symmetric filament of radius $R = 1 \times 10^{18}\,\mathrm{cm}$ (corresponding to $6.5'$). The molecular gas density in the filament is assumed to be independent of the radius r and equal to $n_g = n_0 \cos\alpha$. To obtain the appropriate linear mass density we put $n_0 = 3 \times 10^3\,\mathrm{cm}^{-3}$. The extinction in the central parts of the filament is then found to take the reasonable value of 6.4 mag. It is also assumed that T_g and T_i are independent of r. The magnetic field is supposed to be helical with the components given by

$$B_\varphi = B_{\varphi 0} \frac{r}{R} \tag{14}$$

$$B_z = B_{z0} \left(1 - \frac{r^2}{R^2}\right) \quad . \tag{15}$$

This field resembles the field of Model I but the B_z-component here varies more smoothly implying an electric current in the φ-direction that is more distributed across the filament. The maximum strength of the magnetic field is taken to be $B_{max} = 12\,\mu\mathrm{G}$ (Heiles 1988; Myers & Goodman 1988).

Using Eq. (12) we have numerically calculated the polarization in the model filament for a great number of different sets of parameter values. Just as in Model I the angle of polarization takes only the values 0° and 90° in the absence of a background/foreground polarization. Flips between these angles may also occur. Fig. 6 shows the polarization for $\kappa = 0.3$, $\alpha = 0^\circ$, $T_i = 8\,\mathrm{K}$, $\Delta T = T_g - T_i = 5\,\mathrm{K}$, and the paired quantities $P_V(0)/A_V = 0.16$, $C_1 = 10$ and $P_V(0)/A_V = 0.08$, $C_1 = 48$ (cf. Sect. 5.2). The two lower curves give the polarization in case of no background/foreground polarization. All the polarization vectors are perpendicular to the filament. It is to be noticed that, in spite of the fact that ΔT has been put as large as 5 K, the maximum polarization in the middle of the filament is limited to about 0.3% for $P_V(0)/A_V = 0.16$, $C_1 = 10$ and to barely 0.6% for $P_V(0)/A_V = 0.08$, $C_1 = 48$.

The two upper curves in Fig. 6 illustrate the polarization for a similar situation but now with a background/foreground polarization of 2% directed perpendicular to the filament, resembling the polarization observed in the neighbourhood of the

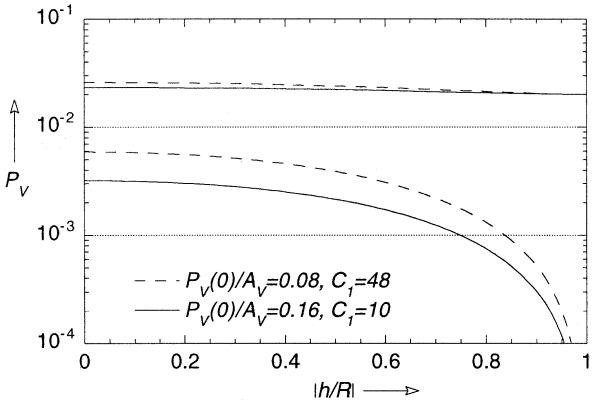

Fig. 6. Polarization P_V in a model of the L204 dark cloud (Model III) shown as a function of $|h/R|$ for $\kappa = 0.3$, $\alpha = 0°$, $T_i = 8$ K, and $\Delta T = 5$ K. The two lower curves illustrate the polarization in case of no background/foreground polarization while the two upper curves show the polarization for a background/foreground polarization of $P_b = 0.02$ perpendicular to the filament.

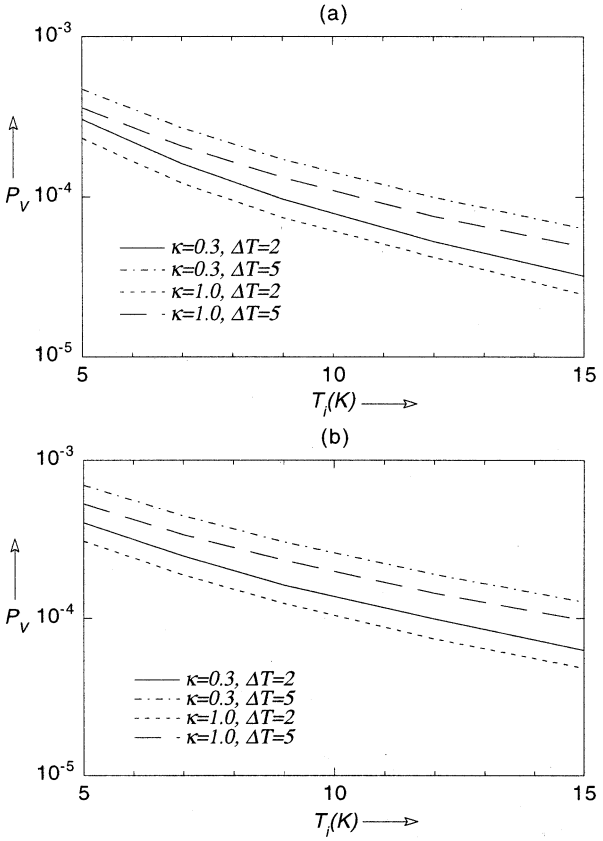

Fig. 7a and b. Polarization P_V at a position where $A_V = 2.5$ mag in Model III as a function of the grain temperature T_i for a few different values of κ and ΔT. The filament is oriented so that $\alpha = 0°$. **a** refers to $P_V(0)/A_V = 0.16$, $C_1 = 10$ while **b** refers to $P_V(0)/A_V = 0.08$, $C_1 = 48$.

L204 dark cloud. Obviously, the filament contributes very little to the total polarization in the cases shown.

By varying B_{max} slightly around the value adopted we have found that the polarization in the filament varies in proportion to B_{max}^{μ} where $\mu \approx 1.4 - 1.8$ (cf. Sect. 3.1).

The polarization has also been determined for filaments which are not perpendicular to the l.o.s. For reasonable values of α the polarization differs only moderately from the polarization obtained in the perpendicular case. For a filament where e.g. $\kappa = 0.3$, $T_i = 10$ K, and $\Delta T = 5$ K, seen at an angle of $\alpha = 30°$, the polarization at $h/R = 0$ is larger by a factor ~ 1.2 compared with the polarization of a similar filament seen at an angle $\alpha = 0°$.

As mentioned above the polarization has hitherto been measured only in the outer parts of the L204 cloud. For the sake of comparison we have calculated the polarization at $|h/R| \approx 0.92$, where $A_V = 2.5$ mag, for a few different values of κ, T_i, and ΔT. The results are summed up in Fig. 7. It is found that nowhere in the diagram does the polarization exceed 0.1%.

Similarly we have calculated the polarization in the central parts of a filament using $\kappa = 0.3$, $\alpha = 0°$, $\Delta T = 5$ K, $P_V(0)/A_V = 0.08$, and $C_1 = 48$. For reasonable grain temperatures around 10 K (Greenberg 1978; Draine & Lee 1984) the polarization is $\sim 0.4\%$. If instead the grain temperature would be as low as 5 K the polarization may amount to $\sim 1.2\%$.

It should be recognized that the radial distribution of many of the physical quantities, associated with the L204 cloud, are not very well known. It is therefore relevant to ask oneself how the choice of distributions influences the polarization. In order to elucidate this question we have studied a few other filamentary models of the L204 cloud with more complex distributions. Common to the models is that they comprise a helical magnetic field and the same values of the linear density and B_{max} as those considered above. Numerical calculations show that the polarization in these models does not differ significantly from the polarization found in the simple model above. Hence, it may be concluded that the polarization is not very sensitive to the choice of distributions.

6. Discussion

We have studied the polarization and extinction of light in three models of filamentary molecular clouds. For the cylindrically symmetric Models I and III we have shown that, in the absence of a background/foreground polarization, the angle of polarization has a bimodal character assuming either 0° or 90°. For certain κ-values both of these angles can exist simultaneously in one and the same filament. The transition between the two angles is then abrupt. If a background/foreground polarization is present or if, as in Model II, the filament is not cylindrically symmetric, polarization angles others than 0° and 90° will in general also exist.

In this connection it may be of some interest to notice that in some molecular clouds like the Perseus dark cloud complex (Goodman et al. 1990) and the Ophiuchus dark cloud complex, especially the B42 region (Vrba et al. 1988), the observed angle of polarization has a bimodal character similar to that in Models

I and III. Is the reason for this bimodal character of the molecular clouds the same as that for the models? From our study a necessary condition for a positive answer is that the background/foreground polarization must be relatively small so that the molecular clouds account for the main part of the polarization observed, amounting to at least a few percent.

We may compare this requirement with the polarization estimated by means of Model III. For extinctions $A_V \leq 2.5$ mag in the cloud we get a polarization well below 0.1% (cf. Fig. 7). Only for an extinction of more than six magnitudes and for very low values of the grain temperature and the parameter $P_V(0)/A_V$ the polarization exceeds one percent. Hence, we conclude that molecular clouds of the kind studied here most likely contribute very little to the polarization observed.

This conclusion agrees very well with the view recently put forward by Goodman et al. (1992, 1995). From near-infrared (J, H, K) polarimetry in the elongated molecular clouds B216–217 and L1755 they find that the polarization vectors in the denser parts of the clouds ($1 \lesssim A_V \lesssim 10$) have about the same direction as those in the more dilute parts ($A_V \lesssim 1$). In the L1755 cloud the polarization vectors are almost aligned with the long axis of the cloud while in the B216–217 cloud they are about perpendicular to this axis. The distributions of the polarization position angles measured at optical and near-infrared wavelengths are nearly identical. Moreover, the polarization is not found to increase with the extinction. The properties of the B216–217 cloud are in many respects similar to those of the L204 cloud. We have calculated the polarization for a model of the B216–217 cloud assuming it to be of cylindrical shape. We find, just as for the L204 cloud, that the polarization caused by the B216–217 cloud is small compared with the polarization actually observed.

Summing up we find that it is not a straightforward task to figure out the geometry of the magnetic field in filamentary molecular clouds like the L204 cloud from polarization measurements. First, the background/foreground polarization is expected to dominate the polarization caused by the filament itself. Secondly, even in the absence of a background/foreground polarization the magnetic field line pattern might be very different from the polarization pattern. We therefore conclude that the assumption of a helical magnetic field inside filamentary molecular clouds like the L204 cloud is not in conflict with the results of the polarimetric measurements performed. A better method for finding out the geometry of the magnetic field might be to study more carefully the fine structure of the filamentary clouds which has a tendency to be aligned with the ambient magnetic field (Carlqvist & Gahm 1992). This method is certainly not very well suited for determining the strength of the magnetic field but may offer a good opportunity of finding the structure of the field.

Acknowledgements. We wish to thank G.F. Gahm and R. Liseau for stimulating discussions and for many valuable suggestions. We also would like to thank the referee, P.G. Martin, whose constructive comments have contributed very much to this paper.

References

Alfvén H., Carlqvist P., 1978, Ap&SS 54, 279
Bohlin R.C., Savage B.D., Drake J.F., 1978, ApJ 224, 132
Brinks E., 1990, In: Thronson H.A. Jr., Shull J.M. (eds.) The Interstellar Medium in Galaxies. Kluwer, Dordrecht, p. 39
Carlqvist P., 1988, Ap&SS 144, 73
Carlqvist P., Gahm G.F., 1992, IEEE Trans. Plasma Sci. 20, 867
Davis L. Jr., Greenstein J.L., 1951, ApJ 114, 206
Draine B.T., Hyung Mok Lee, 1984, ApJ 285, 89
Goodman A.A., Bastien P., Myers P.C., Ménard F., 1990, ApJ 359, 363
Goodman A.A., Jones T.J., Lada E.A., Myers P.C., 1992, ApJ 399, 108
Goodman A.A., Jones T.J., Lada E.A., Myers P.C., 1995, ApJ 448, 748
Goodman A.A., Whittet D.C.B., 1995, ApJ 455, L181
Greenberg J.M., 1969, Physica 41, 67
Greenberg J.M., 1978, In: McDonnell J.A.M. (ed.) Cosmic Dust. John Wiley & Sons, New York, p. 187
Heiles C., 1988, ApJ 324, 321
Heyer M.H., Vrba F.J., Snell R.L. et al., 1987, ApJ 321, 855
Jones R.V., Spitzer L. Jr., 1967, ApJ 147, 943
Kalberla P.M.W., Schwarz U.J., Goss W.M., 1985, A&A 144, 27
Kim S.-H., Martin P.G., 1995, ApJ 444, 293
Knapp G.R., 1990, In: Thronson H.A. Jr., Shull J.M. (eds.) The Interstellar Medium in Galaxies. Kluwer, Dordrecht, p. 3
Kulkarni S.R., Heiles C., 1987, In: Hollenbach D.J., Thronson H.A. Jr. (eds.) Interstellar Processes. Reidel, Dordrecht, p. 87
Langer W.D., 1978, ApJ 225, 95
Lynds B.T., 1962, ApJS 7, 1
Martin P.G., 1974, ApJ 187, 461
Martin P.G., 1975, ApJ 202, 393
Martin P.G., 1995, ApJ 445, L63
Mathis J.S., 1986, ApJ 308, 281
McCutcheon W.H., Vrba F.J., Dickman R.L., Clemens D.P., 1986, ApJ 309, 619 (MVDC)
McGregor P.J., Harrison T.E., Hough J.H., Bailey J.A., 1994, MNRAS 267, 755
Moneti A., Pipher J.L., Helfer H.L., McMillan R.S., Perry M.L., 1984, ApJ 282, 508
Myers P.C., Goodman A.A., 1988, ApJ 326, L27
Myers P.C., Goodman A.A., 1991, ApJ 373, 509
Purcell E.M., 1979, ApJ 231, 404
Serkowski K., Chojnacki W., Rueinski S., 1967, In: Greenberg J.M., Roark T.P. (eds.) Interstellar Grains. NASA SP-140, 51
Serkowski K., Mathewson D.S., Ford V.L., 1975, ApJ 196, 261
Spitzer L. Jr., 1978, Physical Processes in the Interstellar Medium. John Wiley & Sons, New York, p. 187
Spitzer L. Jr., 1985, Physica Scripta T11, 5
Spitzer L. Jr., Tukey J.W., 1951, ApJ 114, 187
Tamura M., Nagata T., Sato S., Tanaka M., 1987, MNRAS 224, 413
Vrba F.J., Coyne G.V., Tapia S., 1981, ApJ 243, 489
Vrba F.J., Strom S.E., Strom K.M., 1988, AJ 96, 680

This article was processed by the author using Springer-Verlag LaTeX A&A style file *L-AA* version 3.